Available online at www.sciencedirect.com

ScienceDirect

Procedia Structural Integrity 28 (2020) 2350–2369

Structural Integrity Procedia

www.elsevier.com/locate/procedia

1st Virtual European Conference on Fracture

A physically consistent virtual crack closure technique accounting for contact and interpenetration

Paolo S. Valvo[a,*]

[a]*University of Pisa, Department of Civil and Industrial Engineering, Largo Lucio Lazzarino, I-56122 Pisa, PI, Italy*

Abstract

In some circumstances, the standard formulation of the virtual crack closure technique (VCCT) may yield negative values of the modal contributions to the energy release rate. To avoid such physically meaningless results, a revised formulation is available. However, the revised VCCT does not take into account possible interpenetration of the crack faces, that may be predicted by the linearly elastic solution. The present work extends the revised VCCT formulation by introducing suitable contact constraints to prevent local interpenetration of the crack-tip nodes. By considering open vs. interpenetrated cracks and tensile vs. compressive crack-tip forces, four cases emerge. For each case, a suitable two-step crack closure process is outlined with the two steps respectively corresponding to fracture modes II and I. The contact pressure force, if present, is evaluated and accounted for in the computation of the crack closure work. As a result, novel analytical expressions are derived for the modal contributions to the energy release rate accounting for contact and prevented interpenetration.

Keywords:

1. Introduction

The virtual crack closure technique (VCCT) is a numerical method used to compute the energy release rate, $\mathcal{G}$, in the finite element analysis of fracture mechanics problems [Krueger (2004)]. The technique was introduced first for two-dimensional problems by Rybicki and Kanninen (1977). Later, the VCCT was extended to three-dimensional problems by Shivakumar et al. (1988). For mixed-mode fracture problems, such as the delamination of composite materials and interfacial fracture, the VCCT furnishes not only the total $\mathcal{G}$, but also the contributions, $\mathcal{G}_{\mathrm{I}}$, $\mathcal{G}_{\mathrm{II}}$, and $\mathcal{G}_{\mathrm{III}}$, associated to the three basic fracture modes [Krueger et al. (2013)].

* Corresponding author. Tel.: +39-050-2218223.
E-mail address: p.valvo@ing.unipi.it

10.1016/j.prostr.2020.11.083

Nomenclature

a	crack length
B	crack width = out-of-plane thickness of cracked body
c_{xx}	crack-tip flexibility coefficient = relative displacement in x-direction due to unit forces in x-direction
c_{xz}	crack-tip flexibility coefficient = relative displacement in x-direction due to unit forces in z-direction
c_{zx}	crack-tip flexibility coefficient = relative displacement in z-direction due to unit forces in x-direction
c_{zz}	crack-tip flexibility coefficient = relative displacement in z-direction due to unit forces in z-direction
C	position of crack tip
C^-	position of crack tip on bottom crack face
C^+	position of crack tip on top crack face
$\mathbf{C}$	crack-tip flexibility matrix
D	position of propagated crack tip
F_x	crack-tip force in x-direction
F_x^c	crack-tip force in x-direction at local contact
F_z	crack-tip force in z-direction
F_z^c	crack-tip force in z-direction at local contact
$\mathbf{F}$	crack-tip force vector
$\mathcal{G}$	energy release rate
$\mathcal{G}_{\mathrm{I}}$	mode I contribution to energy release rate
$\mathcal{G}_{\mathrm{II}}$	mode II contribution to energy release rate
k_{xx}	crack-tip stiffness coefficient = nodal force in x-direction due to unit displacement in x-direction
k_{xz}	crack-tip stiffness coefficient = nodal force in x-direction due to unit displacement in z-direction
k_{zx}	crack-tip stiffness coefficient = nodal force in z-direction due to unit displacement in x-direction
k_{zz}	crack-tip stiffness coefficient = nodal force in z-direction due to unit displacement in z-direction
$\mathbf{K}$	crack-tip stiffness matrix
p	distributed contact pressure
q_x	distributed crack closure force in x-direction
q_z	distributed crack closure force in z-direction
Q_x	crack closure force in x-direction
Q_x^{I}	mode I crack closure force in x-direction
Q_x^{II}	mode II crack closure force in x-direction
$Q_x^{\mathrm{II,a}}$	mode II crack closure force in x-direction, sub-step a
$Q_x^{\mathrm{II,b}}$	mode II crack closure force in x-direction, sub-step b
Q_z	crack-tip closure force in z-direction
Q_z^{I}	mode I crack closure force in z-direction
Q_z^{II}	mode II crack closure force in z-direction
$Q_z^{\mathrm{II,a}}$	mode II crack closure force in z-direction, sub-step a
$Q_z^{\mathrm{II,b}}$	mode II crack closure force in z-direction, sub-step b
O	origin of reference system
x	Cartesian coordinate
$\bar{x}$	direction of crack-tip force vector corresponding to contact
z	Cartesian coordinate
$\bar{z}$	direction of crack-tip force vector corresponding to mode I fracture
Γ	ellipse of crack-tip flexibility
Δa	crack length increment
ΔA	crack area increment
Δu_x	crack-tip relative displacement in x-direction
Δu_x^c	crack-tip relative displacement in x-direction at local contact

Δu_x^{I} mode I crack-tip relative displacement in x-direction
Δu_x^{II} mode II crack-tip relative displacement in x-direction
$\Delta u_x^{\mathrm{II,a}}$ mode II crack-tip relative displacement in x-direction, sub-step a
$\Delta u_x^{\mathrm{II,b}}$ mode II crack-tip relative displacement in x-direction, sub-step b
Δu_z crack-tip relative displacement in z-direction
Δu_z^c crack-tip relative displacement in z-direction at local contact
Δu_z^{I} mode I crack-tip relative displacement in z-direction
Δu_z^{II} mode II crack-tip relative displacement in z-direction
$\Delta u_z^{\mathrm{II,a}}$ mode II crack-tip relative displacement in z-direction, sub-step a
$\Delta u_z^{\mathrm{II,b}}$ mode II crack-tip relative displacement in z-direction, sub-step b
$\Delta \mathbf{u}$ crack-tip relative displacement vector
ΔW crack closure work
ΔW_{I} mode I crack closure work
ΔW_{II} mode II crack closure work
σ_z normal stress on crack plane
τ_{xz} shear stress on crack plane

Focusing on I/II mixed-mode fracture problems, Valvo (2012) demonstrated that the standard VCCT may be inappropriate to analyse problems involving highly asymmetric cracks. In fact, physically unacceptable, negative values for either $\mathcal{G}_{\mathrm{I}}$ or $\mathcal{G}_{\mathrm{II}}$ may be calculated. The origin of this shortcoming was identified in the lack of energetic orthogonality between the Cartesian components of the crack-tip force used to calculate the modal contributions. Thereafter, Valvo (2015) proposed a physically consistent, revised VCCT, whereas the crack-tip force is decomposed into the sum of two energetically orthogonal systems of forces. As a result, always non-negative $\mathcal{G}_{\mathrm{I}}$ and $\mathcal{G}_{\mathrm{II}}$ are obtained. Equivalently, the modal contributions to $\mathcal{G}$ can be associated to the amounts of work done in a suitable two-step process of crack closure. The technique was extended also to three-dimensional problems involving I/II/III mixed-mode fracture by Valvo (2014).

The revised VCCT has been applied successfully to analyse a number of practical fracture problems involving, e.g., adhesive joints [Sengab and Talreja (2016)], composite beams [Jang and Ahn (2018)], rubber tires [Kelliher (2018)], and multidirectional fibre-reinforced laminates [Garulli et al. (2020)].

The VCCT can be regarded as the numerical implementation of the crack closure integral introduced by Irwin (1958). Accordingly, the energy release rate is calculated based on the hypothesis that the energy spent in propagating the crack is equal to the work that would be done to close the crack by suitable crack closure forces. For open cracks, the crack closure forces are equal to the stresses acting on the crack faces prior to crack propagation. Nevertheless, there are cases, in which the elastic solution predicts contact and interpenetration between the crack faces. In such cases, the crack closure forces must take into account the presence of contact pressures [Laursen (2002)].

The present work extends the previous formulation of the revised VCCT for I/II mixed-mode problems, by introducing suitable contact constraints to prevent local interpenetration of the crack-tip nodes. Depending on the presence of interpenetration and compressive forces normal to the crack plane, four cases are identified:

1. open crack in tension;
2. open crack in compression;
3. interpenetrated crack in compression;
4. interpenetrated crack in tension.

The open crack in tension is essentially the case considered by Valvo (2015). The other three cases are analysed here for the first time.

The paper is organised as follows. In Section 2, Irwin (1958)'s crack closure integral is briefly recalled together with a short discussion on its possible modification in the presence of contact pressures. In Section 3, a finite element discretisation of the fracture problem is introduced with particular reference to some concepts introduced by Valvo

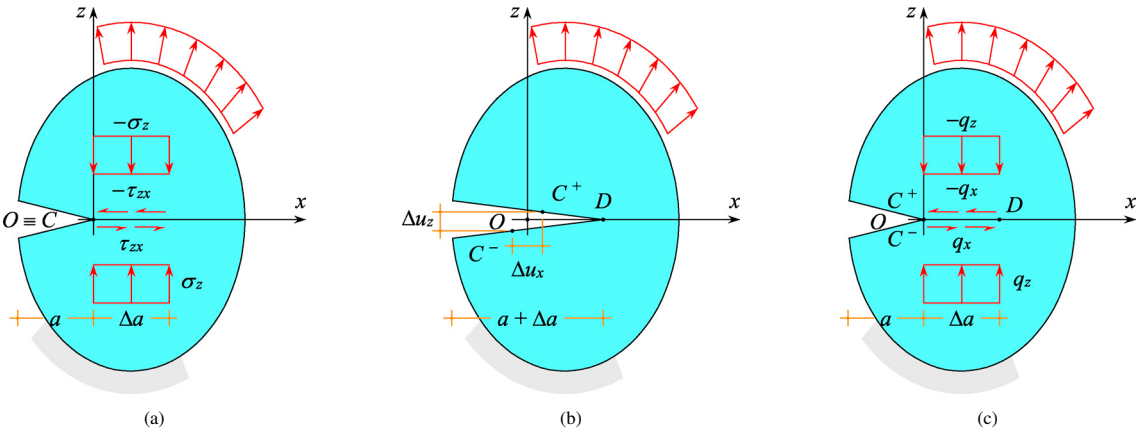

Fig. 1: Crack closure integral for an open crack: (a) initial crack; (b) crack propagation; (c) crack closure.

(2012): the crack-tip flexibility coefficients and the ellipse of crack-tip flexibility. In Section 4, the revised virtual crack closure technique is presented: for each of the above-mentioned four cases, a suitable crack closure process enabling fracture mode decomposition is defined. Thus, analytical expressions are derived for the modal contributions to the energy release rate. In Section 5, some conclusive remarks are given together with directions for future developments.

2. Crack closure integral

2.1. Open crack

Let us consider a planar elastic body with a straight crack of initial length a. A Cartesian reference system, Oxz, is placed in the body plane with the origin, O, placed at the initial position of the crack tip, C, and the x-axis aligned with the initial crack direction (Fig. 1a). The material is supposed to be linearly elastic under either plane stress or plane strain conditions [Timoshenko and Goodier (1951)].

Irwin (1958) observed that the energy spent for crack propagation is equal to the work necessary to close the extended crack by suitable forces. For an open crack, i.e. when the elastic solution does not predict any interpenetration of the crack faces (Fig. 1b), the forces needed to close the crack are exactly the same as the stresses acting on the (bonded) crack faces prior to crack propagation.

Let us imagine that the crack propagates by a small length, Δa, with the initial crack tip, C, splitting into two new points, C^- and C^+, and with a new crack-tip position, D, on the x-axis. To close the crack and restore the initial situation, distributed forces equal to the stresses initially acting on the segment CD should be applied,

$$\begin{aligned} q_x(x) &= \tau_{xz}(x), \\ q_z(x) &= \sigma_z(x), \end{aligned} \tag{1}$$

where $\sigma_z(x)$ and $\tau_{xz}(x)$ are the normal and shear stresses acting on the bonded part of the crack plane, respectively.

The actual work done to close the crack is equal to half the virtual work of the distributed crack closure forces,

$$\Delta W = \frac{1}{2} B \int_0^{\Delta a} \left[q_x(x)\, \Delta u_x(x) + q_z(x)\, \Delta u_z(x) \right] \mathrm{d}x, \tag{2}$$

where $\Delta u_x(x)$ and $\Delta u_z(x)$ are the relative displacement between the crack faces in the x- and z-directions, respectively, and B is the thickness of the cracked body in the out-of-plane direction.

The energy release rate is calculated as the work done per unit area of new crack surface in the limit for a vanishing crack propagation length:

$$\mathcal{G} = \lim_{\Delta a \to 0} \frac{\Delta W}{\Delta A}, \tag{3}$$

where $\Delta A = B\,\Delta a$ is the area of new crack surface created.

By substituting Eqs. (1) and (2) into (3), we obtain:

$$\mathcal{G} = \frac{1}{2} \lim_{\Delta a \to 0} \frac{1}{\Delta a} \int_0^{\Delta a} \left[\tau_{xz}(x)\,\Delta u_x(x) + \sigma_z(x)\,\Delta u_z(x) \right] \mathrm{d}x. \tag{4}$$

For symmetric cracks, the two addends in Eq. (4) correspond to the contributions of fracture modes I and II:

$$\begin{aligned} \mathcal{G}_{\mathrm{I}} &= \frac{1}{2} \lim_{\Delta a \to 0} \frac{1}{\Delta a} \int_0^{\Delta a} \sigma_z(x)\,\Delta u_z(x)\ \mathrm{d}x, \\ \mathcal{G}_{\mathrm{II}} &= \frac{1}{2} \lim_{\Delta a \to 0} \frac{1}{\Delta a} \int_0^{\Delta a} \tau_{xz}(x)\,\Delta u_x(x)\ \mathrm{d}x. \end{aligned} \tag{5}$$

It should be observed that the simple fracture mode partitioning expressed by Eqs. (5) originates from the splitting of the stress field into the sum of a symmetric part (mode I) and an antisymmetric part (mode II) with respect to the crack plane. This partitioning is not valid in general for asymmetric and bimaterial interface cracks.

2.2. Interpenetrated crack

Now, let us consider the possible case, in which the elastic solution predicts interpenetration of the crack faces as a consequence of crack propagation. When the initial crack of length a (Fig. 2a) propagates by a small length, Δa, some overlap occurs in the neighbourhood of the crack tip (Fig. 2b). Indeed, this overlap is prevented by the development of a contact pressure, $p(x)$, along the interface. Assuming frictionless contact between the crack faces, the contact pressure will act in the direction normal to the crack plane (Fig. 2c). As a consequence, the forces needed to close the crack and restore the initial situation should be evaluated by properly accounting for such contact pressure (Fig. 2d):

$$\begin{aligned} q_x(x) &= \tau_{xz}(x) \\ q_z(x) &= \sigma_z(x) + p(x). \end{aligned} \tag{6}$$

In theory, Eq. (6) may be substituted into (2) to compute the energy release rate. In practice, however, the determination of $p(x)$, such that $\Delta u_z(x) = 0$, may be quite difficult and an analytical treatment of problem may be unfeasible. In what follows, we will develop a numerical implementation of the local contact problem in the simplifying assumption that only the crack-tip nodes experience some overlap.

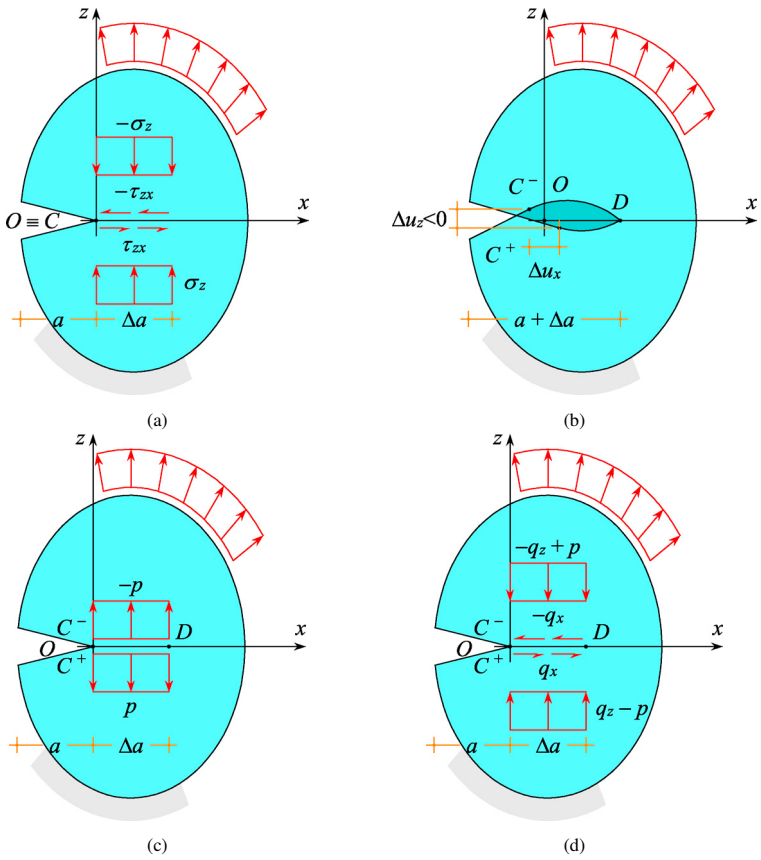

Fig. 2: Crack closure integral in the event of crack face interpenetration: (a) initial crack; (b) crack propagation with interpenetration; (c) crack propagation with contact; (d) crack closure accounting for contact forces.

3. Finite element discretisation

3.1. Finite crack propagation

Let us now consider a finite element discretisation of the elasticity problem outlined in the previous Section. For the sake of simplicity, we consider four-noded plane stress/plane strain elements of constant thickness B, but extension to different types of elements is possible [Krueger (2004)].

Figure 3a shows a detail of the finite element mesh in the neighbourhood of the crack tip. Here, the crack has the initial length a and the crack tip coincides with nodes C^- and C^+, bonded together and located on the bottom and top crack faces, respectively. Through the crack tip node, concentrated forces are exchanged between the connected elements. We denote with F_x and F_z the forces applied by the top part of the body onto node C^- and with the opposite quantities the forces applied by the bottom part onto node C^+. In the finite element context, such forces play the role of the distributed stresses, $\tau_{xz}(x)$ and $\sigma_z(x)$, of the continuous elasticity problem. Next, crack propagation is considered by a small length, Δa, here equal to the size of the elements connected at the crack tip. Hence, the crack tip moves to node D, while nodes C^- and C^+ undergo the relative displacements Δu_x and Δu_z along the x- and z-axes, respectively (Fig. 3b).

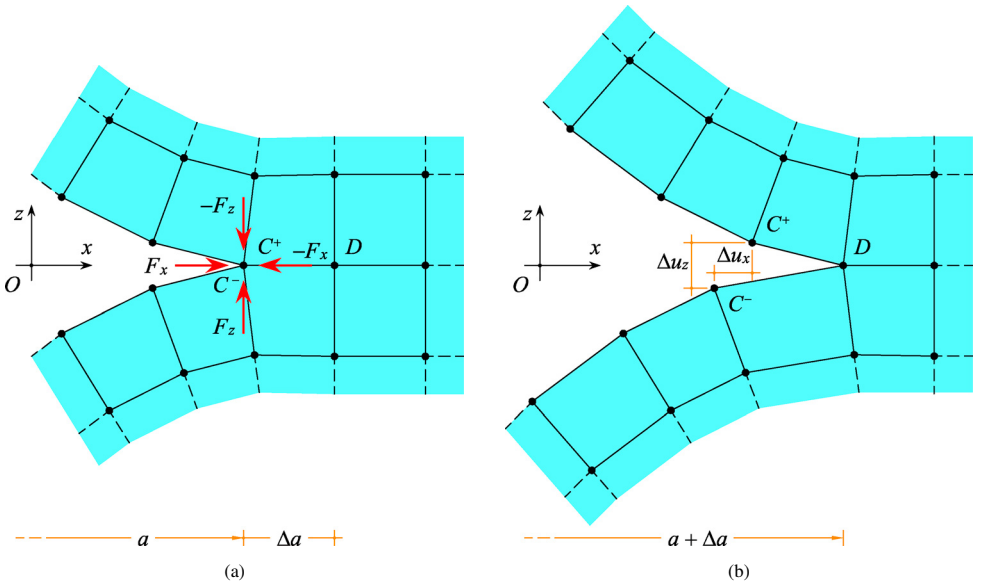

Fig. 3: Virtual crack closure technique: (a) initial crack; (b) crack propagation.

3.2. *Crack-tip flexibility coefficients*

The magnitude of the crack-tip forces may be evaluated by introducing suitable tie constraints into the model, e.g. springs with "infinite" (i.e. numerically large) stiffness between nodes C^- and C^+. As an alternative, the crack-tip forces can be evaluated as follows. We define the crack-tip flexibility coefficients as the relative displacements occurring between the crack tip nodes, C^- and C^+, when the body is subject to unit force loads at the same nodes [Jerram (1970)]. In particular, we denote with c_{xx} and c_{zx} the flexibility coefficients corresponding to the relative displacement in the x- and z-directions, respectively, produced by unit force loads in the x-direction (Fig. 4a). Besides, we denote with c_{xz} and c_{zz} the flexibility coefficients corresponding to the relative displacement in the x- and z-directions, respectively, produced by unit force loads in the z-direction (Fig. 4b). By virtue of Betti's theorem, it is $c_{zx} = c_{xz}$. The above definition can be used also for practical calculation of the flexibility coefficients by carrying out two separate auxiliary analyses on the finite element mesh with the propagated crack [Valvo (2012)].

Because of linearity, the relative displacements produced by general (not unit) crack-tip forces are:

$$\begin{aligned} \Delta u_x &= c_{xx} F_x + c_{xz} F_z, \\ \Delta u_z &= c_{zx} F_x + c_{zz} F_z. \end{aligned} \tag{7}$$

Inversion of Eqs. (7) furnishes:

$$\begin{aligned} F_x &= k_{xx} \Delta u_x + k_{xz} \Delta u_z, \\ F_z &= k_{zx} \Delta u_x + k_{zz} \Delta u_z, \end{aligned} \tag{8}$$

where k_{xx}, $k_{xz} = k_{zx}$, and k_{zz} are stiffness coefficients, whose expressions are given by Eqs. (A.1) in the Appendix.

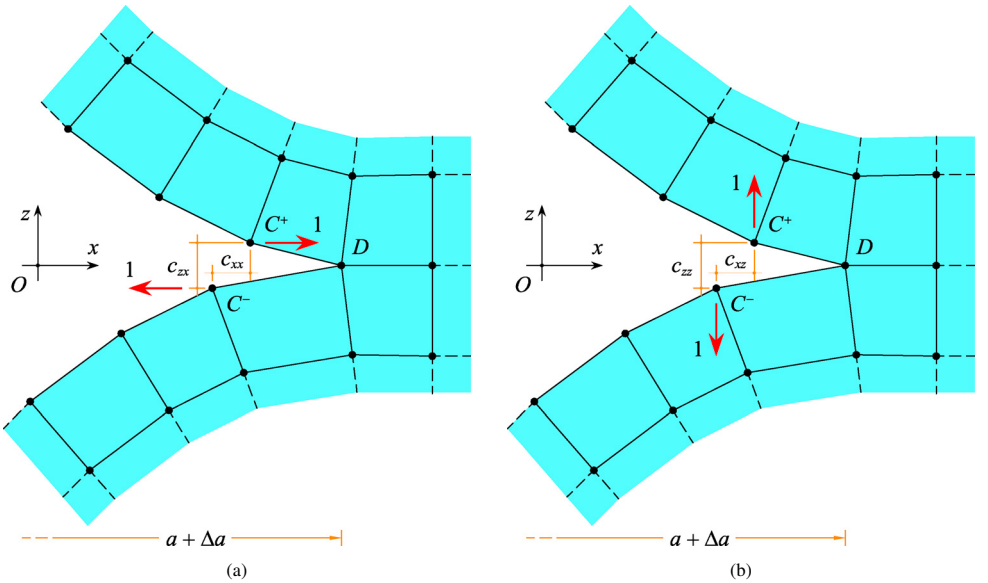

Fig. 4: Flexibility coefficients: (a) unit force loads in the x-direction; (b) unit force loads in the z-direction.

3.3. Matrix notation

It is useful to introduce a more compact matrix notation. We define the crack-tip force vector,

$$\mathbf{F} = \begin{Bmatrix} F_x \\ F_z \end{Bmatrix}, \tag{9}$$

the crack-tip relative displacement vector,

$$\Delta\mathbf{u} = \begin{Bmatrix} \Delta u_x \\ \Delta u_z \end{Bmatrix}, \tag{10}$$

and the crack-tip flexibility matrix (symmetric and positive definite),

$$\mathbf{C} = \begin{bmatrix} c_{xx} & c_{xz} \\ c_{zx} & c_{zz} \end{bmatrix}. \tag{11}$$

Equation (7) becomes simply

$$\Delta\mathbf{u} = \mathbf{C}\,\mathbf{F}\,. \tag{12}$$

A crack-tip stiffness matrix (symmetric and positive definite) can be defined as the inverse of the flexibility matrix,

$$\mathbf{K} = \begin{bmatrix} k_{xx} & k_{xz} \\ k_{zx} & k_{zz} \end{bmatrix} = \mathbf{C}^{-1}. \tag{13}$$

Inversion of Eq. (12) furnishes the matrix version of Eq. (8):

$$\mathbf{F} = \mathbf{K}\,\Delta\mathbf{u}. \tag{14}$$

3.4. Ellipse of crack-tip flexibility

The conical section Γ associated with matrix $\mathbf{C}$ is defined by the following equation:

$$c_{xx}\,x^2 + 2c_{xz}\,xz + c_{zz}\,z^2 = 1. \tag{15}$$

Γ turns out to be an ellipse, here called the ellipse of crack-tip flexibility (Fig. 5). The ellipse helps visualising the relationship between the directions of the crack-tip force vector, $\mathbf{F}$, and relative displacement vector, $\Delta\mathbf{u}$. Namely, it can be demonstrated that $\Delta\mathbf{u}$ has the direction of the outer normal to the ellipse at the point of intersection with the direction of $\mathbf{F}$ [Valvo (2012)]. Two particular directions can be identified:

1. the $\bar{x}$-axis, corresponding to a relative displacement vector, $\Delta\mathbf{u}$, parallel to the x-axis: when $\mathbf{F}$ has the direction of $\bar{x}$, the relative displacement in the z-direction is $\Delta u_z = 0$, which means that contact between the crack faces (at nodes C^- and C^+) is established;

2. the $\bar{z}$-axis, corresponding to a relative displacement vector, $\Delta\mathbf{u}$, parallel to the z-axis: when $\mathbf{F}$ has the direction of $\bar{z}$, the relative displacement in the x-direction is $\Delta u_x = 0$, which means that pure mode I fracture conditions are met.

When $\mathbf{F}$ falls below the x-axis (red and orange regions in Fig. 5), a compressive force, F_z, is expected at the crack-tip node in the direction normal to the crack plane (in the configuration with the initial crack). When $\mathbf{F}$ falls below the $\bar{x}$-axis (orange and yellow regions in Fig. 5), interpenetration of the crack faces is expected (in the configuration with the propagated crack). When $\mathbf{F}$ falls above both the x- and $\bar{x}$-axes (white region in Fig. 5), a tensile force at the crack tip and an open propagated crack are expected.

4. Revised virtual crack closure technique

Based on the above, when computing the crack closure forces to evaluate the energy release rate by the virtual crack closure technique, four cases have to be considered:

1. open crack ($\Delta u_z \geq 0$) in tension ($F_z \geq 0$), corresponding to the white region in Fig. 5;

2. open crack ($\Delta u_z \geq 0$) in compression ($F_z < 0$), corresponding to the red region in Fig. 5;

3. interpenetrated crack ($\Delta u_z < 0$) in compression ($F_z < 0$), corresponding to the orange region in Fig. 5;

4. interpenetrated crack ($\Delta u_z < 0$) in tension ($F_z \geq 0$), corresponding to the yellow region in Fig. 5.

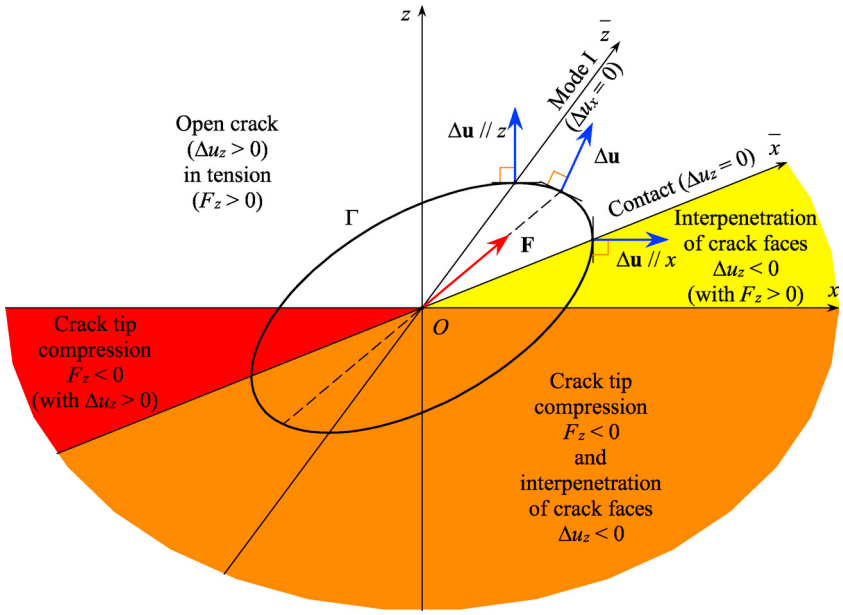

Fig. 5: Ellipse of crack-tip flexibility.

4.1. Open crack in tension

4.1.1. Energy release rate

If $F_z \geq 0$ and $\Delta u_z \geq 0$, the normal crack-tip force is tensile and crack faces will open upon propagation (Fig. 3b). The crack can be closed by applying crack closure forces, Q_x and Q_z, equal to the forces acting prior to crack propagation (Fig. 6):

$$\begin{aligned} Q_x &= F_x, \\ Q_z &= F_z; \end{aligned} \tag{16}$$

The crack closure work is:

$$\Delta W = \frac{1}{2} \left(Q_x \, \Delta u_x + Q_z \, \Delta u_z \right). \tag{17}$$

and the energy release rate turns out to be:

$$\mathcal{G} = \frac{\Delta W}{B \, \Delta a} = \frac{Q_x \, \Delta u_x}{2B \, \Delta a} + \frac{Q_z \, \Delta u_z}{2B \, \Delta a}. \tag{18}$$

It is worth noting that Eqs. (17) and (18) are the discrete versions of (2) and (4), respectively. Likewise, the two addends in Eq. (18) can be regarded as the mode II and I contributions, respectively, but only for symmetric cracks. Nonetheless, the standard VCCT [Krueger (2004)] always assumes this simplistic mode partitioning, which may lead to physically unacceptable, negative values of $\mathcal{G}_{\mathrm{I}}$ and $\mathcal{G}_{\mathrm{II}}$. The origin of this shortcoming has been found to reside in

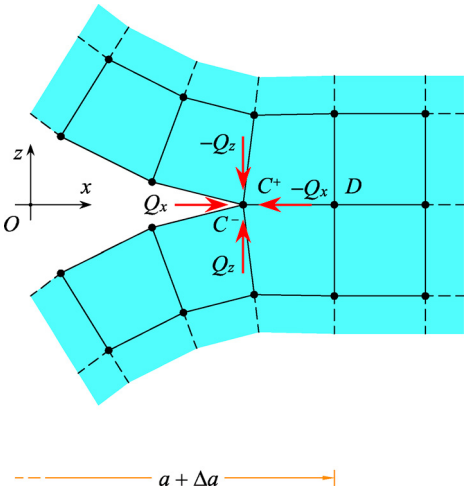

Fig. 6: Crack closure forces for an open crack.

the lack of energetic orthogonality between the Cartesian components of the crack closure forces, Q_x and Q_z. In fact, the work done by Q_x on the displacements produced by Q_z is generally nonzero, and vice versa. Such mutual work is undefined in sign and can add negatively to the amounts of work used to compute the modal contribution to $\mathcal{G}$ [Valvo (2012)].

By substituting Eqs. (8) and (16) into (18), the following expression of the energy release rate for an open crack is obtained:

$$\mathcal{G} = \frac{1}{2B\,\Delta a}\left(k_{xx}\Delta u_x^2 + 2k_{xz}\Delta u_x\Delta u_z + k_{zz}\Delta u_z^2\right). \tag{19}$$

4.1.2. Fracture mode partitioning

A physically consistent fracture mode partitioning can be established by suitably decomposing the crack closure force into the sum of two energetically orthogonal systems of forces, i.e. having null mutual work. To this aim, let us start with the following decomposition of the crack closure force components into mode I and mode II contributions:

$$\begin{aligned} Q_x &= Q_x^{\mathrm{I}} + Q_x^{\mathrm{II}}, \\ Q_z &= Q_z^{\mathrm{I}} + Q_z^{\mathrm{II}}. \end{aligned} \tag{20}$$

Correspondingly, the crack-tip relative displacements are decomposed as:

$$\begin{aligned} \Delta u_x &= \Delta u_x^{\mathrm{I}} + \Delta u_x^{\mathrm{II}}, \\ \Delta u_z &= \Delta u_z^{\mathrm{I}} + \Delta u_z^{\mathrm{II}}, \end{aligned} \tag{21}$$

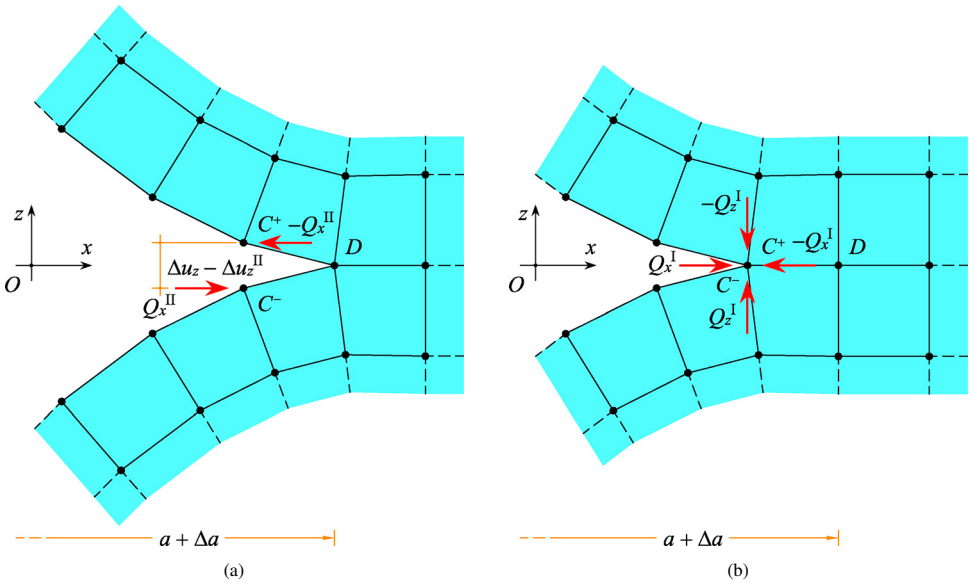

Fig. 7: Two-step closure of an open crack: (a) mode II; (b) mode I.

where, by virtue of Eqs. (7), the mode I contributions to the relative displacements are

$$\begin{aligned} \Delta u_x^{\mathrm{I}} &= c_{xx} Q_x^{\mathrm{I}} + c_{xz} Q_z^{\mathrm{I}}, \\ \Delta u_z^{\mathrm{I}} &= c_{zx} Q_x^{\mathrm{I}} + c_{zz} Q_z^{\mathrm{I}}; \end{aligned} \tag{22}$$

and the mode II contributions are

$$\begin{aligned} \Delta u_x^{\mathrm{II}} &= c_{xx} Q_x^{\mathrm{II}} + c_{xz} Q_z^{\mathrm{II}}, \\ \Delta u_z^{\mathrm{II}} &= c_{zx} Q_x^{\mathrm{II}} + c_{zz} Q_z^{\mathrm{II}}. \end{aligned} \tag{23}$$

According to the revised VCCT [Valvo (2015)], pure mode I is defined as corresponding to a null component of the crack-tip relative displacement in the x-direction ($\Delta u_x^{\mathrm{I}} = 0$). Besides, pure mode II is associated to a null component of the crack closure force in the z-direction ($Q_z^{\mathrm{II}} = 0$). This definition assures the energetic orthogonality between the two systems of crack closure forces, hence a positive definition of $\mathcal{G}_{\mathrm{I}}$ and $\mathcal{G}_{\mathrm{II}}$. The two modal contributions can be associated to the amounts of work done in a two-step process of closure of the propagated crack.

In the first crack closure step, corresponding to mode II (Fig. 7a), the gap between the crack-tip nodes, C^+ and C^-, in the x-direction is completely closed, while no force is applied in the z-direction:

$$\begin{aligned} Q_z^{\mathrm{II}} &= 0, \\ \Delta u_x^{\mathrm{II}} &= \Delta u_x. \end{aligned} \tag{24}$$

By introducing Eqs. (24) into (23), and recalling Eqs. (A.2), the mode II crack closure force in the x-direction and relative displacement in the z-direction are obtained:

$$\begin{aligned} Q_x^{\mathrm{II}} &= \frac{1}{c_{xx}}\Delta u_x = \frac{k_{xx}k_{zz}-k_{xz}^2}{k_{zz}}\Delta u_x, \\ \Delta u_z^{\mathrm{II}} &= \frac{c_{zx}}{c_{xx}}\Delta u_x = -\frac{k_{xz}}{k_{zz}}\Delta u_x. \end{aligned} \tag{25}$$

In the second crack closure step, corresponding to mode I (Fig. 7b), the remainders of the crack closure forces, Eqs. (16), are applied:

$$\begin{aligned} Q_x^{\mathrm{I}} &= Q_x - Q_x^{\mathrm{II}}, \\ Q_z^{\mathrm{I}} &= Q_z - Q_z^{\mathrm{II}}. \end{aligned} \tag{26}$$

By substituting Eqs. (24) and (25) into (26), and recalling Eqs. (8) and (16), we obtain:

$$\begin{aligned} Q_x^{\mathrm{I}} &= \frac{k_{xz}}{k_{zz}}\left(k_{xz}\Delta u_x + k_{zz}\Delta u_z\right), \\ Q_z^{\mathrm{I}} &= k_{xz}\Delta u_x + k_{zz}\Delta u_z. \end{aligned} \tag{27}$$

By substituting Eqs. (27) into (22), and simplifying, the mode I crack-tip relative displacements are deduced:

$$\begin{aligned} \Delta u_x^{\mathrm{I}} &= 0, \\ \Delta u_z^{\mathrm{I}} &= \frac{k_{xz}}{k_{zz}}\Delta u_x + \Delta u_z. \end{aligned} \tag{28}$$

The amounts of work done by the mode I and II systems of crack closure forces respectively are

$$\begin{aligned} \Delta W_{\mathrm{I}} &= \frac{1}{2}Q_z^{\mathrm{I}}\Delta u_z^{\mathrm{I}}, \\ \Delta W_{\mathrm{II}} &= \frac{1}{2}Q_x^{\mathrm{II}}\Delta u_x^{\mathrm{II}}. \end{aligned} \tag{29}$$

Correspondingly, the modal contributions to the energy release rate are

$$\begin{aligned} \mathcal{G}_{\mathrm{I}} &= \frac{\Delta W_{\mathrm{I}}}{B\,\Delta a}, \\ \mathcal{G}_{\mathrm{II}} &= \frac{\Delta W_{\mathrm{II}}}{B\,\Delta a}. \end{aligned} \tag{30}$$

By substituting Eqs. (24), (25), (27), and (28) into (30), the expressions of the modal contributions to the energy release rate for an open crack in tension are finally obtained:

$$\begin{aligned} \mathcal{G}_{\mathrm{I}} &= \frac{1}{2B\,\Delta a}\frac{1}{k_{zz}}\left(k_{xz}\Delta u_x + k_{zz}\Delta u_z\right)^2, \\ \mathcal{G}_{\mathrm{II}} &= \frac{1}{2B\,\Delta a}\frac{k_{xx}k_{zz}-k_{xz}^2}{k_{zz}}\Delta u_x^2. \end{aligned} \tag{31}$$

Eqs. (31) are equivalent to the expressions given by Valvo (2015). It can also be proved that the sum of the two modal contributions is equivalent to the total $\mathcal{G}$ as given by Eq. (19).

4.2. Open crack in compression

In the previous Subsection, it has been tacitly assumed that the crack closure forces applied in the first and second steps do not produce interpenetration of the crack faces. In the first crack closure step, this requires $\Delta u_z^{\mathrm{II}} \le \Delta u_z$ (since the crack is open, $\Delta u_z \ge 0$). From the second of Eqs. (25), and recalling Eqs. (8), this condition can be proven equivalent to the following:

$$F_z = k_{zx}\Delta u_x + k_{zz}\Delta u_z \ge 0, \tag{32}$$

which is always satisfied for an open crack in tension. As concerns the second crack closure step, the non-interpenetration condition, $\Delta u_z^{\mathrm{I}} = \Delta u_z - \Delta u_z^{\mathrm{II}} \ge 0$, is then automatically satisfied.

However, for an open crack in compression, $F_z < 0$. Thus, Eq. (32) is not satisfied. The first crack closure step, corresponding to mode II, must be split into two sub-steps:

(a) a first sub-step, where the crack faces are open and a crack closure force, $Q_x^{\mathrm{II,a}}$, is applied in the x-direction, while $Q_z^{\mathrm{II,a}} = 0$; the sub-step ends when contact is achieved between the crack-tip nodes, C^- and C^+, in the z-direction, which implies $\Delta u_z^{\mathrm{II,a}} = \Delta u_z$; at the same time, the gap between the crack-tip nodes in the x-direction is partly closed by an amount $\Delta u_x^{\mathrm{II,a}}$ (Fig. 8a);

(b) a second sub-step, where the crack faces are in contact ($\Delta u_z^{\mathrm{II,b}} = 0$) and a contact pressure force, $P = -Q_z^{\mathrm{II,b}} > 0$, develops; besides, a crack closure force in the x-direction, $Q_x^{\mathrm{II,b}}$, is applied to close the residual gap between C^- and C^+ in the x-direction, $\Delta u_x^{\mathrm{II,b}} = \Delta u_x - \Delta u_x^{\mathrm{II,a}}$ (Fig. 8b).

More in detail, adaptation of Eqs. (8) for the first sub-step yields

$$\begin{aligned} Q_x^{\mathrm{II,a}} &= k_{xx}\Delta u_x^{\mathrm{II,a}} + k_{xz}\Delta u_z^{\mathrm{II,a}} = k_{xx}\Delta u_x^{\mathrm{II,a}} + k_{xz}\Delta u_z, \\ Q_z^{\mathrm{II,a}} &= k_{zx}\Delta u_x^{\mathrm{II,a}} + k_{zz}\Delta u_z^{\mathrm{II,a}} = 0. \end{aligned} \tag{33}$$

Hence,

$$\begin{aligned} Q_x^{\mathrm{II,a}} &= -\frac{k_{xx}k_{zz}-k_{xz}^2}{k_{xz}}\Delta u_z, \\ \Delta u_x^{\mathrm{II,a}} &= -\frac{k_{zz}}{k_{xz}}\Delta u_z. \end{aligned} \tag{34}$$

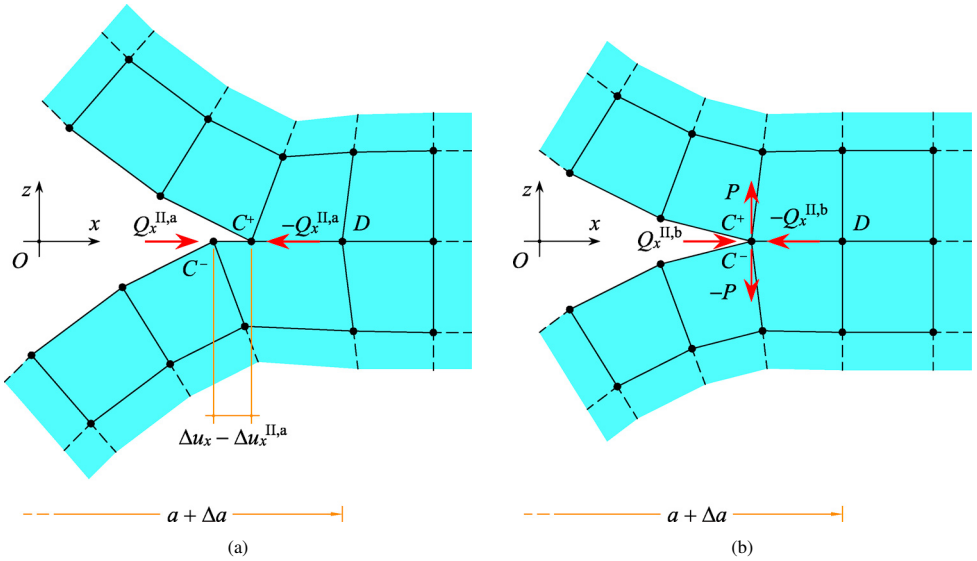

Fig. 8: Mode II closure of an open crack in compression: (a) first sub-step; (b) second sub-step.

For the second sub-step, we have

$$\begin{aligned} Q_x^{\mathrm{II,b}} &= k_{xx}\Delta u_x^{\mathrm{II,b}} + k_{xz}\Delta u_z^{\mathrm{II,b}} = k_{xx}\left(\Delta u_x - \Delta u_x^{\mathrm{II,a}}\right), \\ Q_z^{\mathrm{II,b}} &= k_{zx}\Delta u_x^{\mathrm{II,b}} + k_{zz}\Delta u_z^{\mathrm{II,b}} = -P. \end{aligned} \tag{35}$$

Hence, by recalling previous expressions and simplifying,

$$\begin{aligned} Q_x^{\mathrm{II,b}} &= \frac{k_{xx}}{k_{xz}}\left(k_{xz}\Delta u_x + k_{zz}\Delta u_z\right), \\ \Delta u_x^{\mathrm{II,b}} &= \Delta u_x + \frac{k_{zz}}{k_{xz}}\Delta u_z, \\ P &= -k_{zx}\Delta u_x - k_{zz}\Delta u_z = -F_z. \end{aligned} \tag{36}$$

The work done by $Q_x^{\mathrm{II,a}}$ and $Q_x^{\mathrm{II,b}}$ in the above described sub-steps is to be ascribed entirely to mode II (the contact force does not produce any work as $\Delta u_z^{\mathrm{II,b}} = 0$). By using Eqs. (34) and (36), and simplifying, we obtain

$$\Delta W_{\mathrm{II}} = \frac{1}{2}\left(Q_x^{\mathrm{II,a}} + Q_x^{\mathrm{II,b}}\right)\left(\Delta u_x^{\mathrm{II,a}} + \Delta u_x^{\mathrm{II,b}}\right) = \frac{1}{2}\left(k_{xx}\Delta u_x + k_{xz}\Delta u_z\right)\Delta u_x. \tag{37}$$

At the end of the second sub-step, the crack turns out to be completely closed. Thus, the second crack closure step, corresponding to mode I, is not necessary for an open crack in compression. Hence, a null mode I crack closure work is considered for this case, $\Delta W_{\mathrm{I}} = 0$.

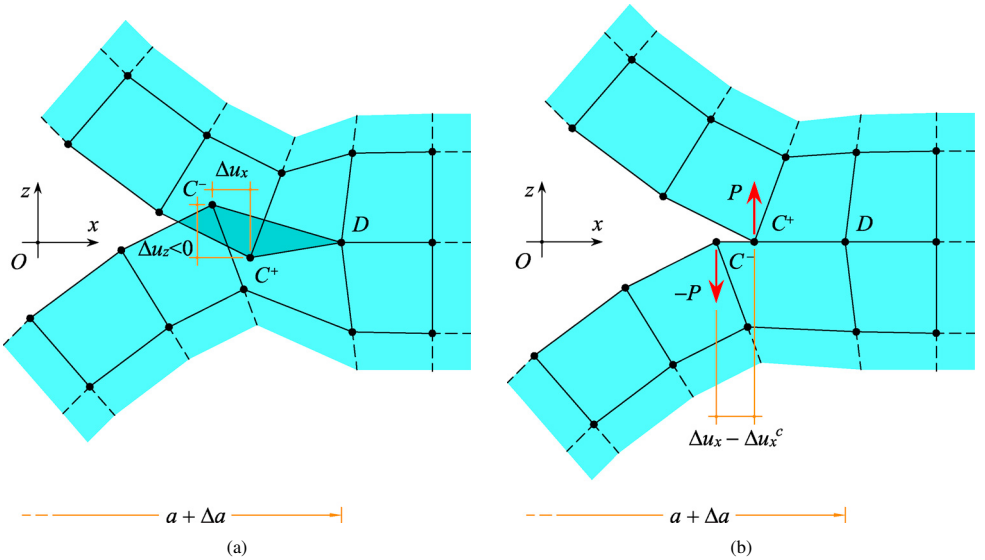

Fig. 9: Interpenetrated crack: (a) theoretical overlap; (b) contact pressure force.

By recalling Eqs. (30), the final expressions of the modal contributions to the energy release rate for an open crack in compression are obtained:

$$\begin{aligned} \mathcal{G}_{\mathrm{I}} &= 0, \\ \mathcal{G}_{\mathrm{II}} &= \frac{1}{2B\,\Delta a}\left(k_{xx}\Delta u_x + k_{xz}\Delta u_z\right)\Delta u_x. \end{aligned} \tag{38}$$

4.3. Interpenetrated crack in compression

In some cases, the elastic solution predicts a theoretical overlap of the crack faces, in particular between the crack-tip nodes with $\Delta u_z < 0$ (Fig. 9a). In practice, such overlap is prevented by the development of contact pressures. Here, we assume that local contact is limited to the crack-tip nodes, C^- and C^+, which exchange a contact pressure force, P (Fig. 9b).

The magnitude of the contact pressure force may be estimated as follows. Let us consider a system of crack-tip forces representing frictionless local contact between the crack faces:

$$\begin{aligned} F_x^c &= 0, \\ F_z^c &= -P. \end{aligned} \tag{39}$$

The corresponding relative displacements can be obtained by substituting Eqs. (39) into (7):

$$\begin{aligned} \Delta u_x^c &= c_{xx}F_x^c + c_{xz}F_z^c = -c_{xz}P, \\ \Delta u_z^c &= c_{zx}F_x^c + c_{zz}F_z^c = -c_{zz}P. \end{aligned} \tag{40}$$

Then, by imposing $\Delta u_z^c = \Delta u_z$, and recalling also Eqs. (A.2), we get

$$\begin{aligned} \Delta u_x^c &= \frac{c_{xz}}{c_{zz}}\Delta u_z \quad = -\frac{k_{xz}}{k_{xx}}\Delta u_z, \\ P \quad &= -\frac{1}{c_{zz}}\Delta u_z = -\frac{k_{xx}k_{zz} - k_{xz}^2}{k_{xx}}\Delta u_z, \end{aligned} \tag{41}$$

which show that a positive contact pressure force ($P > 0$) arises for interpenetrated cracks ($\Delta u_z < 0$).

Again, the modal contributions to $\mathcal{G}$ can be evaluated by imagining a two-step process of crack closure. In the first step, corresponding to mode II (Fig. 10), a crack closure force in the x-direction, Q_x^{II}, is applied to close the gap in the same direction between the crack-tip nodes, C^- and C^+. Differently from the open crack case, such gap must account for the contribution due to contact, so that $\Delta u_x^{\mathrm{II}} = \Delta u_x - \Delta u_x^c$. Besides, a crack closure force in the z-direction, Q_z^{II}, is added to the contact pressure force, P. to make sure that the two crack faces be in contact throughout the crack closure step, i.e. $\Delta u_z^{\mathrm{II}} = 0$. Thus, adaptation of Eqs. (8) yields

$$\begin{aligned} Q_x^{\mathrm{II}} \quad &= k_{xx}\Delta u_x^{\mathrm{II}} + k_{xz}\Delta u_z^{\mathrm{II}} = k_{xx}\left(\Delta u_x - \Delta u_x^c\right), \\ Q_z^{\mathrm{II}} - P &= k_{zx}\Delta u_x^{\mathrm{II}} + k_{zz}\Delta u_z^{\mathrm{II}} = k_{zx}\left(\Delta u_x - \Delta u_x^c\right). \end{aligned} \tag{42}$$

By substituting Eqs. (41) into (42), and simplifying, we get

$$\begin{aligned} Q_x^{\mathrm{II}} \quad &= k_{xx}\Delta u_x + k_{xz}\Delta u_z = F_x, \\ Q_z^{\mathrm{II}} - P &= k_{zx}\Delta u_x + k_{zz}\Delta u_z = F_z. \end{aligned} \tag{43}$$

The crack closure work related to mode II is

$$\Delta W_{\mathrm{II}} = \frac{1}{2}Q_x^{\mathrm{II}}\Delta u_x^{\mathrm{II}} = \frac{1}{2}\frac{1}{k_{xx}}\left(k_{xx}\Delta u_x + k_{xz}\Delta u_z\right)^2. \tag{44}$$

Eqs. (43) show that at the end of the first crack closure step, the total crack-tip forces acting in the initial configuration are applied. Therefore, there is no need for a second crack closure step, corresponding to mode I, and the related crack closure work is $\Delta W_{\mathrm{I}} = 0$. By recalling Eqs. (30), the modal contributions to the energy release rate for an interpenetrated crack in compression become

$$\begin{aligned} \mathcal{G}_{\mathrm{I}} &= 0, \\ \mathcal{G}_{\mathrm{II}} &= \frac{1}{2B\,\Delta a}\frac{1}{k_{xx}}\left(k_{xx}\Delta u_x + k_{xz}\Delta u_z\right)^2. \end{aligned} \tag{45}$$

4.4. Interpenetrated crack in tension

The deductions of the previous section are valid as long as a compressive force in the z-direction is present throughout the crack closure step. This requires $Q_z^{\mathrm{II}} - P < 0$ or, by virtue of the second of Eqs. (43), $F_z < 0$, which clearly holds for an interpenetrated crack in compression.

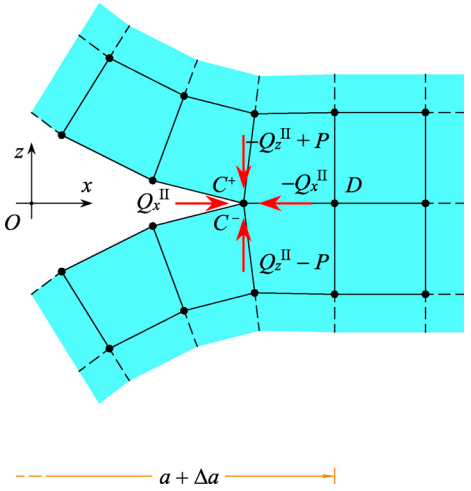

Fig. 10: Crack closure forces for an interpenetrated crack in compression.

For an interpenetrated crack ($\Delta u_z < 0$) in tension ($F_z \geq 0$), a different derivation is required. The crack is again closed in two steps. In the first step, corresponding to mode II, a crack closure force in the x-direction is applied to close the gap in the same direction, $\Delta u_x^{\mathrm{II}} = \Delta u_x - \Delta u_x^c$. The initial contact pressure force, P, decreases gradually until it vanishes at some point. Afterwards, the crack faces open with null contact force between the crack-tip nodes, C^- and C^+. The final value of the crack closure force in the x-direction, Q_x^{II}, is the same given for an open crack in tension by Eqs. (25). The mode II crack closure work is

$$\Delta W_{\mathrm{II}} = \frac{1}{2} Q_x^{\mathrm{II}} \Delta u_x^{\mathrm{II}} = \frac{1}{2} \frac{k_{xx}k_{zz} - k_{xz}^2}{k_{xx}k_{zz}} \left(k_{xx}\Delta u_x + k_{xz}\Delta u_z\right) \Delta u_x \tag{46}$$

In the second step, corresponding to mode I, the remainders of the crack closure forces are applied. These are equal to the mode I crack closure forces applied for an open crack in tension, Eqs. (27). Also, the associated crack-tip relative displacements are the same as those given by Eqs. (28). As a consequence, the mode I contribution to the energy release rate has the same expression of the first of Eqs. (31).

To sum up, the final expressions of the modal contributions to the energy release rate for an interpenetrated crack in tension are the following:

$$\begin{aligned} \mathcal{G}_{\mathrm{I}} &= \frac{1}{2B\,\Delta a} \frac{1}{k_{zz}} \left(k_{xz}\Delta u_x + k_{zz}\Delta u_z\right)^2 , \\ \mathcal{G}_{\mathrm{II}} &= \frac{1}{2B\,\Delta a} \frac{k_{xx}k_{zz} - k_{xz}^2}{k_{xx}k_{zz}} \left(k_{xx}\Delta u_x + k_{xz}\Delta u_z\right) \Delta u_x . \end{aligned} \tag{47}$$

5. Conclusions

It is now well known that the standard VCCT may yield physically inconsistent, negative values of the modal contributions to the energy release rate. This shortcoming comes out, in particular, when analysing problems of bodies with highly asymmetric cracks [Valvo (2012)].

In the present work, the physically consistent revised VCCT proposed by Valvo (2015) has been extended by introducing contact constraints to prevent interpenetration of the crack faces that may be predicted by the linearly elastic solution. In particular, local contact has been considered between the crack-tip nodes in the finite element

mesh with the propagated crack. The contact pressure force, if present, has been evaluated and accounted for in the computation of the crack closure work. Four cases have emerged from the analysis. For each, a suitable two-step crack closure process has been outlined with the two steps respectively corresponding to fracture modes II and I. Such two-step processes need not be implemented in practice in the numerical method, whereas only the final expressions of the modal contributions to $\mathcal{G}$ can be introduced. These are summarised in Table 1. It is an easy task to verify that all of the obtained expressions furnish positive definite quantities. Besides, it can be verified that continuity is assured between the four sub-domains of definition.

Table 1: Modal contributions to the energy release rate.

Case	Crack-tip relative displacement	Crack-tip force	Modal contributions to the energy release rate
Open crack in tension	$\Delta u_z \geq 0$	$F_z \geq 0$	$\mathcal{G}_{\mathrm{I}} = \frac{1}{2B\,\Delta a}\frac{1}{k_{zz}}\left(k_{xz}\Delta u_x + k_{zz}\Delta u_z\right)^2$ $\mathcal{G}_{\mathrm{II}} = \frac{1}{2B\,\Delta a}\frac{k_{xx}k_{zz}-k_{xz}^2}{k_{zz}}\Delta u_x^2$
Open crack in compression	$\Delta u_z \geq 0$	$F_z < 0$	$\mathcal{G}_{\mathrm{I}} = 0$ $\mathcal{G}_{\mathrm{II}} = \frac{1}{2B\,\Delta a}\left(k_{xx}\Delta u_x + k_{xz}\Delta u_z\right)\Delta u_x$
Interpenetrated crack in compression	$\Delta u_z < 0$	$F_z < 0$	$\mathcal{G}_{\mathrm{I}} = 0$ $\mathcal{G}_{\mathrm{II}} = \frac{1}{2B\,\Delta a}\frac{1}{k_{xx}}\left(k_{xx}\Delta u_x + k_{xz}\Delta u_z\right)^2$
Interpenetrated crack in tension	$\Delta u_z < 0$	$F_z \geq 0$	$\mathcal{G}_{\mathrm{I}} = \frac{1}{2B\,\Delta a}\frac{1}{k_{zz}}\left(k_{xz}\Delta u_x + k_{zz}\Delta u_z\right)^2$ $\mathcal{G}_{\mathrm{II}} = \frac{1}{2B\,\Delta a}\frac{k_{xx}k_{zz}-k_{xz}^2}{k_{xx}k_{zz}}\left(k_{xx}\Delta u_x + k_{xz}\Delta u_z\right)\Delta u_x$

It is worth emphasising that in the present work only a local contact constraint has been considered at the crack-tip nodes. Extensive contact between the crack faces requires a more complex analysis. Future work will be devoted to validate the present technique by comparison with results obtained by introducing extensive contact constraints.

Possible future developments include the evaluation of friction between the crack faces and the extension to three-dimensional I/II/III mixed-mode fracture problems.

Acknowledgements

Financial support from the University of Pisa through the PRA 2018-2019 Project “Multi-scale Modelling in Structural Engineering” is gratefully acknowledged.

Appendix A. Crack-tip stiffness and flexibility coefficients

The stiffness coefficients obtained from inversion of the crack-tip stiffness matrix, Eq. (13), are

$$\begin{aligned} k_{xx} &= \frac{c_{zz}}{c_{xx}c_{zz}-c_{xz}^2}, \\ k_{xz} &= -\frac{c_{xz}}{c_{xx}c_{zz}-c_{xz}^2} = k_{zx}, \\ k_{zz} &= \frac{c_{xx}}{c_{xx}c_{zz}-c_{xz}^2}. \end{aligned} \tag{A.1}$$

Vice versa, the flexibility coefficients can be expressed as functions of the stiffness coefficients as follows:

$$\begin{aligned} c_{xx} &= \frac{k_{zz}}{k_{xx}k_{zz} - k_{xz}^2}, \\ c_{xz} &= -\frac{k_{xz}}{k_{xx}k_{zz} - k_{xz}^2} = c_{zx}, \\ c_{zz} &= \frac{k_{xx}}{k_{xx}k_{zz} - k_{xz}^2}. \end{aligned} \tag{A.2}$$

References

Garulli, T., Catapano, A., Fanteria, D., Jumel, J., Martin, E., 2020. Design and finite element assessment of fully uncoupled multi-directional layups for delamination tests. Journal of Composite Materials 54, 773–790.

Irwin, G.R., 1958. Fracture. In: Flügge, S. (Ed.), "*Handbuch der Physik*", vol. VI. Springer, Berlin, Germany, pp. 551–590.

Jang, J.H., Ahn, S.H., 2018. Computation of energy release rates for composite beam through cross-sectional analysis and virtual crack closure technique. Advanced Composite Materials 27, 615–636,

Jerram, K., 1970. "Discussion on 'Stress intensity factors for a part-circular surface flow' by F.W. Smith and M.J. Alavi," 1st International Conference on Pressure Vessel Technology. Delft, Netherlands. Part III, Discussion, ASME, New York, NY, p. 160.

Kelliher, D.S., 2018. Calculating Energy Release Rate as a Function of Crack Length Using a Multiple-Step Crack Closure Technique in Tire Finite Element Models. Tire Science and Technology 46, 130–152.

Krueger, R., 2004. Virtual crack closure technique: History, approach, and applications. Applied Mechanics Reviews 57, 109–143.

Krueger, R., Shivakumar, K., Raju, I.S., 2013. "Fracture mechanics analyses for interface crack problems – A review," 54th AIAA/ASME/ASCE/AHS/ASC Structures, Structural Dynamics, and Materials Conference. Boston, Article number AIAA 2013-1476.

Laursen, T.A., 2002. "*Computational contact and impact mechanics: fundamentals of modeling interfacial phenomena in nonlinear finite element analysis*". Springer, Berlin.

Rybicki, E.F., Kanninen, M.F. 1977. A finite element calculation of stress intensity factors by a modified crack closure integral. Engineering Fracture Mechanics 9, 931–938.

Sengab, A., Talreja, R., 2016. A numerical study of failure of an adhesive joint influenced by a void in the adhesive. Composite Structures 156, 165–170.

Shivakumar, K.N., Tan, P.W., Newman, J.C., 1988. A virtual crack-closure technique for calculating stress intensity factors for cracked three dimensional bodies. International Journal of Fracture 36, R43–R50.

Timoshenko, S., Goodier, J.N., 1951. "*Theory of Elasticity*". McGraw-Hill, New York, NY.

Valvo, P.S., 2012. A revised virtual crack closure technique for physically consistent fracture mode partitioning. International Journal of Fracture 173, 1–20.

Valvo, P.S., 2014. A physically consistent virtual crack closure technique for I/II/III mixed-mode fracture problems. Procedia Materials Science 3, 1983–1987.

Valvo, P.S., 2015. A further step towards a physically consistent virtual crack closure technique. International Journal of Fracture 192, 235–244.